Journal of Alloys and Compounds 492 (2010) 691–694

Contents lists available at ScienceDirect

Journal of Alloys and Compounds

journal homepage: www.elsevier.com/locate/jallcom

Microstructure and magnetic microstructure of La + Co doped strontium hexaferrites

Zhiyong Pang[a,*], Xijian Zhang[a], Boming Ding[b], Daxin Bao[b], Baoshan Han[c]

[a] School of Physics, State Key Laboratory of Crystal Materials, Shandong University, Shanda South Road 27#, Jinan, Shandong 250100, China
[b] Central Research Institute, HENGDIAN DMEGC MAGNETICS Co., LTD, Dongyang, Zhejiang 322118, China
[c] Institute of Physics, Chinese Academy of Sciences, Beijing 100080, China

ARTICLE INFO

Article history:
Received 15 October 2009
Received in revised form 1 December 2009
Accepted 2 December 2009
Available online 11 December 2009

Keywords:
Permanent magnets
Surfaces and interfaces
Domain structure
Microstructure
Atomic force microscopy

ABSTRACT

After being cut, carefully ground, meticulously polished and properly eroded, the microstructure and magnetic microstructure of $La_{0.3}Sr_{0.7}Fe_{11.8}Co_{0.2}O_{19}$ hexaferrites were investigated by using magnetic force microscopy. The shapes of a large amount of the $La_{0.3}Sr_{0.7}Fe_{11.8}Co_{0.2}O_{19}$ grains were determined to be mostly irregular flat columns. The shape anisotropy of the hexaferrite grains can be explained by an abnormal grain growth process occurs for La + Co-containing hexaferrite powders. The magnetizations mainly align parallel or anti-parallel to the direction of oriented magnetic field. The magnetic domain sizes are in the same order of magnitude with the grain sizes. No complex domain structures like corrugation and spike were observed. Micromagnetic simulations were also performed to help analyzing the magnetic microstructure.

1. Introduction

M-Type hexaferrites have attracted extensive interests partially due to their technological significance in applications such as permanent magnets, microwave devices, magnetic recording media, high-frequency devices and magneto-optical devices [1–3]. In view of the technological significance and the large volume of the market, many attempts have been made to improve the key magnetic properties by various methods such as doping [4,5], heat-treatment [6], SiO_2 addition [7], ion irradiation [8], etc. Doping on the Fe [4,9] or Ba/Sr [10,11] lattices was expected to improve the magnetic properties. It was found, however, that either the saturation magnetization M_s, or the anisotropy field H_A, or both decrease. It was noticed that improved properties could be achieved by simultaneous doping with La and Co [12,13]. Some techniques such as nuclear magnetic resonance (NMR) [12] and Mossbauer [14,15] were employed to investigate La + Co doped *M*-type hexaferrites. Most of the works focused on the structures, magnetic properties, chemical valences or phases. Rare investigation, however, paid attention to the magnetic domain structures.

Magnetic force microscope (MFM) is a powerful instrument to investigate the crystalline and magnetic microstructures of magnetic materials partially due to its high lateral resolution and capability of capturing the crystalline microstructure images and corresponding magnetic microstructure images simultaneously. However, to our knowledge, few investigation on magnetic microstructure of La + Co doped *M*-type hexaferrites by MFM has been reported. A possible reason is that the surface of the as prepared ferrites is very rough, which makes it hard to achieve MFM images. In this paper, after cutting, careful grinding, meticulous polishing and proper eroding of the sample surfaces along and perpendicular to the oriented magnetic field, the microstructure and corresponding magnetic microstructure of La + Co doped strontium hexaferrites were investigated by using MFM. Micromagnetic simulations were also performed to help analyzing the magnetic microstructure.

2. Experimental

Ingots with nominal composition of $La_{0.3}Sr_{0.7}Fe_{11.8}Co_{0.2}O_{19}$ (at.%) were prepared by ceramic process. Pure Fe_2O_3 and $SrCO_3$ were selected as the raw material. A small quantity of La_2O_3 and Co_2O_3 were added while wet blending. The blended materials were calcined at 1200 °C for 1 h, and then ball milled for 25 h. After granulation, the ferrites were pressed in an oriented magnetic field of 12,000 Oe and then sintered at 1210 °C for 1 h with a temperature upgrade speed of 150 °C/h.

The detection of magnetic microstructures and topographic feature of the samples was performed by NanoScope IIIa-D3000 MFM in Tapping/Lift modes. The magnetic probes used were micro-fabricated Si cantilevers with pyramidal tip coated with about 40 nm thick magnetic Co–Cr thin film and they were magnetized

* Corresponding author. Tel.: +86 531 88365435; fax: +86 531 88565435.
E-mail address: pang@sdu.edu.cn (Z. Y. Pang).

0925-8388/$ – see front matter © 2009 Elsevier B.V. All rights reserved.
doi:10.1016/j.jallcom.2009.12.019

downward prior to imaging. In scanning, the tip lift-height was 50 nm and the oscillation frequency of the tips was about 79.6 kHz. The samples for MFM study were cut parallel and perpendicular to the oriented magnetic field. After being carefully grinded and meticulously polished, the samples were vacuum annealed at 450 °C for 1 h to remove the stress built in the surface layer and eroded by hydrochloric acids for about half a minute to visualize the grain boundaries.

3. Results and discussion

The intrinsic coercivity H_{cj}, remnant induction B_r and maxima magnetic energy product $(BH)_{max}$ of the $La_{0.3}Sr_{0.7}Fe_{11.8}Co_{0.2}O_{19}$ hexaferrites are 437.9 kA/m, 429 mT and 35.2 kJ/m^3, respectively.

Fig. 1 shows the topographic images of $La_{0.3}Sr_{0.7}Fe_{11.8}Co_{0.2}O_{19}$ hexaferrites performed by MFM. The scan size is 5 μm × 5 μm. Fig. 1(a) and (b) was achieved on the surfaces perpendicular and parallel to the oriented axis, respectively. It can be seen from the images that the grains mostly, or at least largely, have irregular section shapes of approximate round or hexagon in Fig. 1a and approximate rectangle in Fig. 1b, indicating that the grains in the samples are mostly irregular flat columns. The shape anisotropy of the hexaferrite grains can be explained by an abnormal grain growth process occurs for La + Co-containing hexaferrite powders [16,17]. Moreover, there is another interesting phenomenon seen from Fig. 1b that the rectangle sections have a comparative good alignment with their long axes perpendicular to the oriented field direction. That is, the short one is the easy axis of magnetization. In other words, during ball milling process, the $La_{0.3}Sr_{0.7}Fe_{11.8}Co_{0.2}O_{19}$ hexaferrites are easy to crack in the layer perpendicular to the easy axis of magnetization. Fig. 2 gives corresponding topographic images with large scan sizes of 10 μm × 10 μm. The characters of the $La_{0.3}Sr_{0.7}Fe_{11.8}Co_{0.2}O_{19}$ grains mentioned above can also be clearly recognized. Combined

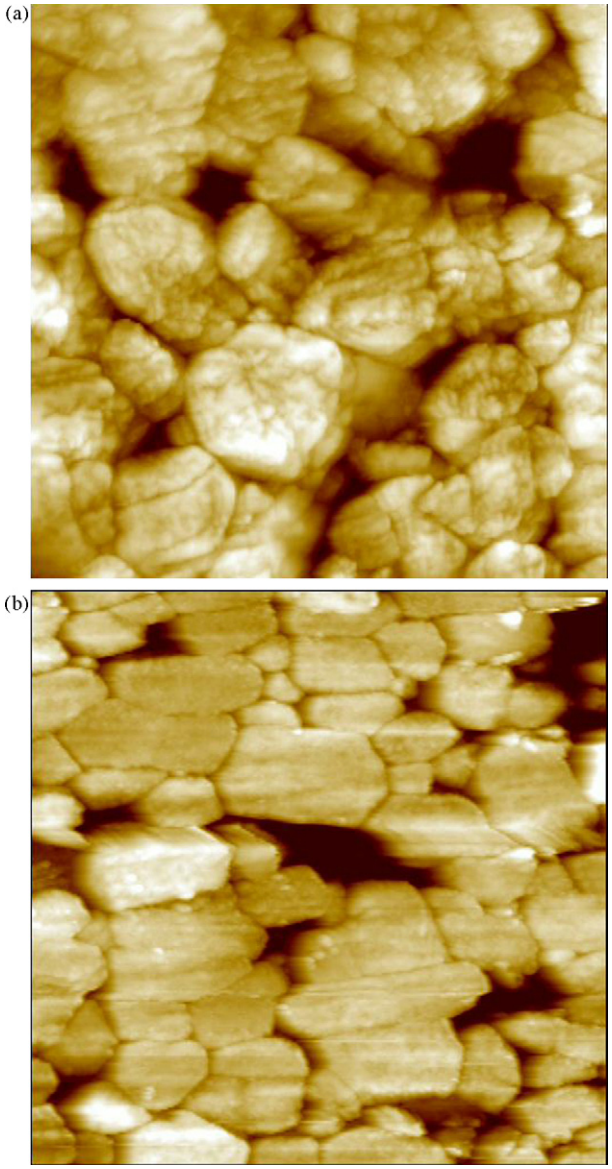

Fig. 1. Topographic images of $La_{0.3}Sr_{0.7}Fe_{11.8}Co_{0.2}O_{19}$ hexaferrites performed by MFM. The scan size is 5 μm × 5 μm and the z range is 200 nm. (a) Images captured on the surfaces perpendicular to the oriented magnetic field; (b) images captured on the surfaces parallel to the oriented magnetic field.

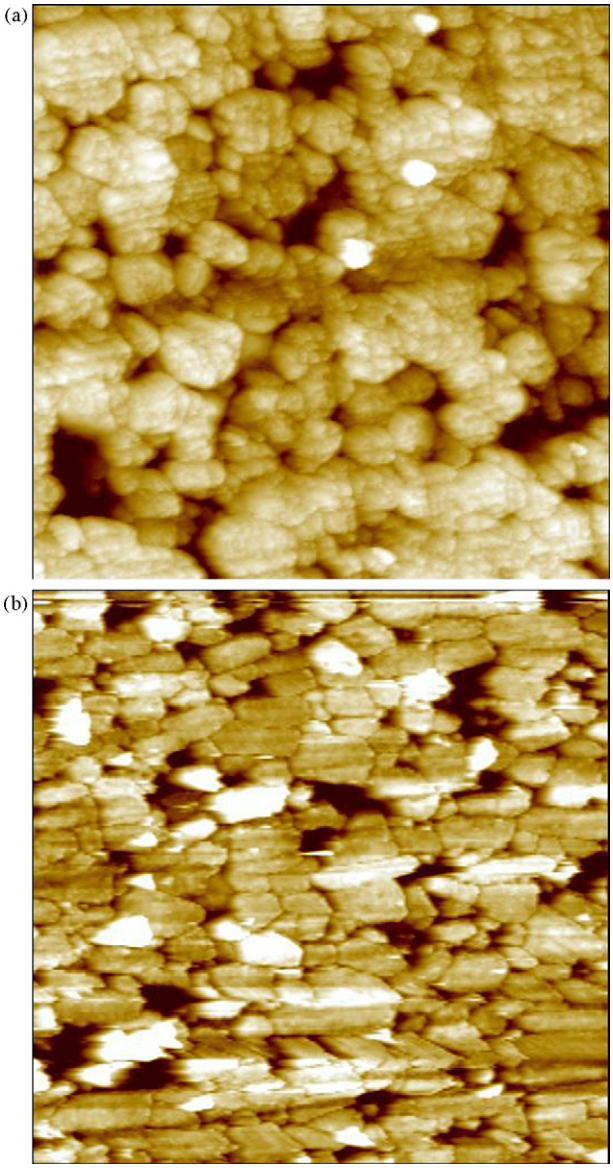

Fig. 2. Topographic images of $La_{0.3}Sr_{0.7}Fe_{11.8}Co_{0.2}O_{19}$ hexaferrites performed by MFM. The scan size is 10 μm × 10 μm and the z range is 200 nm. (a) Images captured on the surfaces perpendicular to the oriented magnetic field; (b) images captured on the surfaces parallel to the oriented magnetic field.

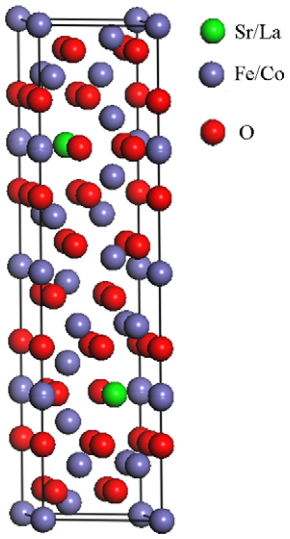

Fig. 3. Unit cell structure of *M*-type strontium hexaferrites.

with the unit cell of *M*-type strontium hexaferrites shown in Fig. 3, it can be deduced that the $La_{0.3}Sr_{0.7}Fe_{11.8}Co_{0.2}O_{19}$ ferrites should be easy to crack in the (0 0 0 1) plane during a ball milling process.

The corresponding magnetic force images of above topographic images are shown in Fig. 4 (5 μm × 5 μm) and Fig. 5 (10 μm × 10 μm), respectively. It can be seen that the magnetic images captured from the plane perpendicular to the oriented magnetic field are characterized by darker areas adjacent to brighter areas, however, large grey areas are observed in the images captured from the surfaces along to the oriented magnetic field, showing that the magnetizations mainly align parallel or antiparallel to the oriented direction [18]. The domain sizes are in the same order of magnitude with the grain sizes (∼several hundred nanometers), showing that the crystal sizes are around the single domain limit. The theoretic single domain limit calculated from the formula:

$$R_0 = \frac{9\gamma_{180^\circ}}{\mu_0 M_S^2} \quad (1)$$

(where γ_{180° is the domain wall energy of 180° wall, M_S is the saturation magnetization) is about 320 nm [19]. This value is very close to the observed experimental domain sizes. Previous research [20] pointed out that both the large and the small grains would reduce the coercivity due to the emergence of multi-domain and superparamagnetism, respectively. However, few experimental observations of single domain limit in La + Co doped strontium hexaferrites have been reported, our experiment provides a basic reference.

No complex domain structures like corrugation and spike which often observed in other hard ferromagnetic materials were observed in our experiments, which maybe because that the grain size less than the critical thickness T_2 ($T_2 = 128\gamma/\mu_0 M_S^2$) [21]. For $La_{0.3}Sr_{0.7}Fe_{11.8}Co_{0.2}O_{19}$ hexaferrites, T_2 is about 5 μm, while the grain size is no thicker than 1 μm. Complex domain structures could not form. Moreover, because the grain sizes great larger than 10 nm, the "exchange coupling domain" [22] exists in nanocomposite magnetic material could not form, either.

The magnetic domain structures of permanent magnets are tightly related to the size and shape of the grains. To well understand the observed magnetic microstructure, micromagnetic simulations were performed and the results shown in Fig. 6. The micromagnetic models used are three dimensional model based on the Object Oriented MicroMagnetic Framework (OOMMF) software available from NIST [23]. The micromagnetic elements are initially assigned a random direction, and the system is allowed to evolve to a stable state. It can be seen from Fig. 6 that for grains with same diameter d = 250 nm, sphere and column with height h = 250 nm are in single domain states. Columns with h = 200 nm and h = 150 nm are in two and three domain states, respectively. Platelet-shaped grains divide into more magnetic domains. To improve the magnetic performance further, it is necessary to reduce the volume fraction of the flat grains and, at the same time, control the crystal sizes just below the single domain limit.

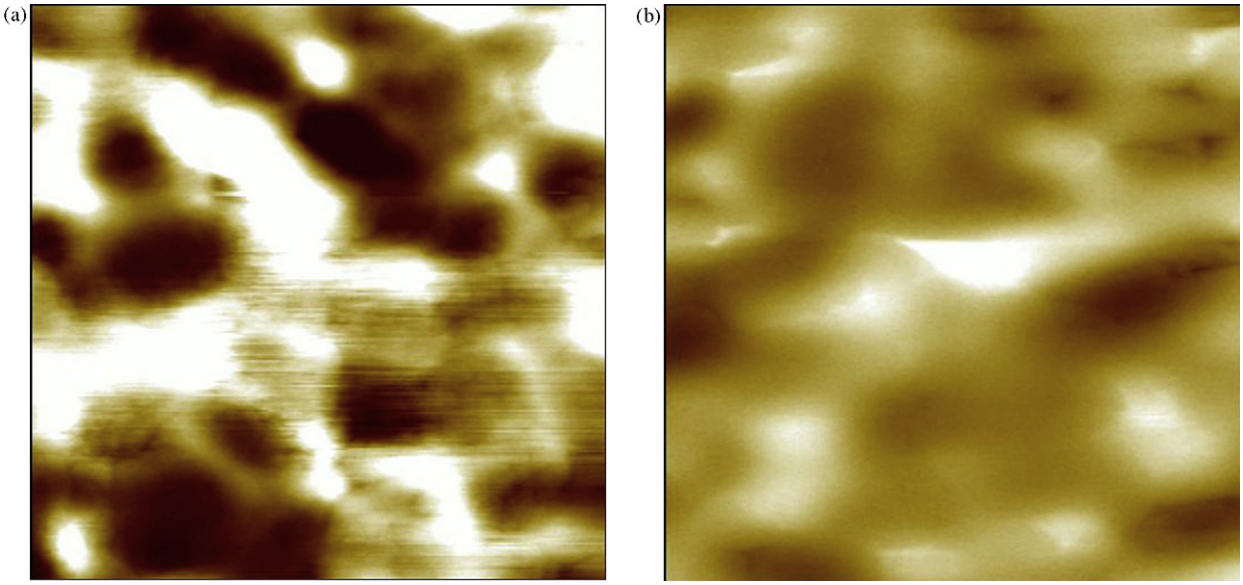

Fig. 4. Magnetic force images of $La_{0.3}Sr_{0.7}Fe_{11.8}Co_{0.2}O_{19}$ hexaferrites performed by MFM. The magnetic force images and the topographic images shown in Fig. 1 are captured in the same place simultaneously. The scan size is 5 μm × 5 μm and the *z* range is 40°. (a) Images captured on the surfaces perpendicular to the oriented magnetic field; (b) images captured on the surfaces parallel to the oriented magnetic field.

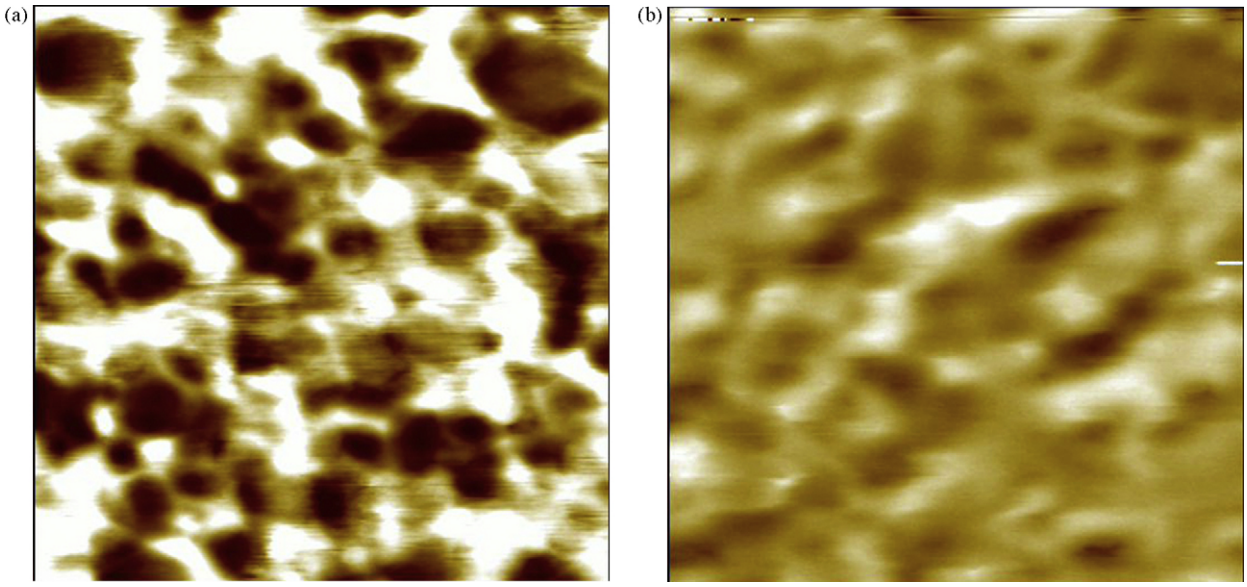

Fig. 5. Magnetic force images of $La_{0.3}Sr_{0.7}Fe_{11.8}Co_{0.2}O_{19}$ hexaferrites performed by MFM. The magnetic force images and the topographic images shown in Fig. 2 are captured in the same place simultaneously. The scan size is 10 μm × 10 μm and the z range is 40°. (a) Images captured on the surfaces perpendicular to the oriented magnetic field; (b) images captured on the surfaces parallel to the oriented magnetic field.

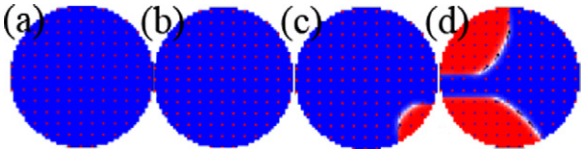

Fig. 6. Micromagnetic simulations of domain states in xy plane. (a) Spheres, d = 250 nm; (b) columns, d = 250 nm and h = 250 nm; (c) columns, d = 250 nm and h = 200 nm; (d) columns, d = 250 nm and h = 150 nm.

4. Conclusions

In summary, the microstructure and corresponding magnetic microstructure of $La_{0.3}Sr_{0.7}Fe_{11.8}Co_{0.2}O_{19}$ hexaferrites are investigated by MFM. The grains are mostly irregular flat columns. During ball milling process, the $La_{0.3}Sr_{0.7}Fe_{11.8}Co_{0.2}O_{19}$ crystals are easy to crack in the (0 0 0 1) plane. The magnetizations mainly align parallel or anti-parallel to the direction of oriented magnetic field. The magnetic domain widths are in the same order of magnitude with the grain sizes. No complex domain structures like corrugation and spike were observed.

Acknowledgements

The authors are grateful for financial support from the Natural Science Foundation of China (Grant no. 60676041 and 10974118), the Shandong Province Natural Science Foundation (Grant no. ZR2009GQ010) and the Scientific and Technological Developing Scheme of Shandong Province (Grant no. 2008GG30004004).

References

[1] S.R. Shinde, R. Ramesh, S.E. Lofland, S.M. Bhagat, S.B. Ogale, R.P. Sharma, T. Venkatesan, Appl. Phys. Lett. 72 (1998) 3443.
[2] S.A. Oliver, S.D. Yoon, I. Kozulin, M.L. Chen, C. Vittoria, Appl. Phys. Lett. 76 (2000) 3612.
[3] A. Vijayalakshmi, N.S. Gajbhiye, J. Appl. Phys. 83 (1998) 400.
[4] A.S. Kamzin, L.P. Ol'khovik, Phys. Solid State 41 (1999) 1658.
[5] A.L. Geiler, A. Yang, X. Zuo, S.D. Yoon, Y. Chen, G.H. Vincent, C. Vittoria, Phys. Rev. Lett. 101 (2008) 067201.
[6] C. Doroftei, E. Rezlescu, P.D. Popa, N. Rezlescu, Cryst. Res. Technol. 41 (2006) 1112.
[7] J. Topfer, S. Schwarzer, S. Senz, D. Hesse, J. Eur. Ceram. Soc. 25 (2005) 1681.
[8] B. Kaur, M. Bhat, F. Licci, R. Kumar, S.D. Kulkarni, P.A. Joy, K.K. Bamzai, P.N. Kotru, J. Magn. Magn. Mater. 305 (2006) 392.
[9] M.V. Kuznetsov, L.F. Barquin, Q.A. Pankhurst, I.P. Parkin, J. Phys. D: Appl. Phys. 32 (1999) 2590.
[10] L. Lechevallier, J.M. Le Breton, J.F. Wang, I.R. Harris, J. Magn. Magn. Mater. 269 (2004) 192.
[11] F.J. Berry, J.F. Marco, C.B. Ponton, K.R. Whittle, J. Mater. Sci. Lett. 20 (2001) 431.
[12] M.W. Pieper, F. Kools, A. Morel, Phys. Rev. B 65 (2002) 184402.
[13] P. Tenaud, A. Morel, F. Kools, J.M. Le Breton, L. Lechevallier, J. Alloy. Compd. 370 (2004) 331.
[14] L. Lechevallier, J.M. Le Breton, J. Teillet, A. Morel, F. Kools, P. Tenaud, Physica B: Condens. Matter 327 (2003) 135.
[15] L. Lechevallier, J.M. Le Breton, J.F. Wang, I.R. Harris, J. Phys.: Condens. Matter 16 (2004) 5359.
[16] A. Morel, F. Kools, P. Tenaud, R. Grössinger, M. Rossignol, Proceedings of the Eighth International Conference on Ferrites, Kyoto, Japan, 18–21 September 2000, 2000, p. 434.
[17] F. Kools, A. Morel, R. Grössinger, J.M. Le Breton, P. Tenaud, J. Magn. Magn. Mater. 242–245 (2002) 1270.
[18] D. Li, B.S. Han, Chin. Phys. Lett. 16 (1999) 333.
[19] For a uniaxial crystal, the single domain limit: $R_0 = 9\gamma_{180^\circ}/\mu_0 M_S^2$, where the domain wall energy of 180° wall: $\gamma_{180^\circ} = 4(K_1 A)^{1/2}$. The magnetic parameters were taken as M_S = 370 kA/m, $K_1 = 3.6 \times 10^5$ J/m^3, $A = 6.6 \times 10^{-12}$ J/m, and R_0 was calculated to be about 320 nm.
[20] A. Goldman, Handbook of Modern Ferromagnetic Materials, Kluwer, Boston, 1999.
[21] C. Kittel, Phys. Rev. 70 (1946) 956.
[22] Z.Y. Pang, Y.K. Fang, H.W. Chang, S.H. Han, B.S. Han, W.C. Chang, Chin. Phys. Lett. 20 (2003) 2033.
[23] M.J. Donohue, D.G. Porter, http://math.nist.gov/oommf. The magnetic parameter M_S = 370 kA/m, $K_1 = 3.6 \times 10^5$ J/m^3, $A = 6.6 \times 10^{-12}$ J/m and z-axis is the easy axis of magnetization. The cell size chosen was 5 nm × 5 nm × 10 nm.